

## SOLUTIONS OF THE PION DISPERSION EQUATION IN THE MEDIUM:

## NEW ASPECTS

V.A.Sadovnikova

Petersburg Nuclear Physics Institute, Gatchina, St.Petersburg 188350, Russia,

tel.812-71-46096, fax.812-71-31963, e-mail: sadovnik@thd.pnpi.spb.ru

Keywords: pion dispersion equation, pion condensation, symmetrical nuclear matter

PACS: 13.75.Gx Pion-baryon interactions; 21.60.Jz Hartree Fock and random-phase approximations; 21.65.+f Nuclear matter

## Abstract

In symmetrical nuclear matter the solutions of pion dispersion equation are investigated in the complex plane of the pion frequency  $\omega$ . There are three well-known branches of solutions on the physical sheet : sound, pion and isobar, at the matter density less than the critical one  $\rho < \rho_c$ . At  $\rho > \rho_c$  the fourth branch appears on the physical sheet. For this branch the condition  $\omega_c^2 \leq 0$  (in general case  $\text{Re } \omega_c^2 \leq 0$ ) takes place. This points out the instability of the ground state which is possibly related to the pion condensation.

## 1 Introduction

Some time ago a bright phenomenon of pion condensation predicted in [1] attracted the common attention and was widely investigated [1]-[4]. The reason for this prediction was the fact that one of the solutions of the pion dispersion equation in medium (let it be called  $\omega_c$ ) turns to zero  $\omega_c^2(k) = 0$  (at some momentum  $k \neq 0$ ) while the density of medium increases [1]. This meant an appearance of excitations with zero energy in medium. In this case the ground state should be reconstructed in correspondence with phase transition.

One variant of reconstruction was to include the pion condensate (taken in one or another form) into the ground state. This resulted in a prediction for pion condensation. A

number of efforts was devoted to the search for this phenomenon. The result of discussions given in the book of A.B.Migdal et. al. [2] was that the pion condensation manifested itself weakly and probably was absent (at least not observed) at normal density. Nevertheless, this phenomenon could influence the equation of state at high densities achieved in heavy ion collisions or neutron stars.

Below, we consider in detail the solutions of pion dispersion equation

$$\omega^2 - k^2 - m_\pi^2 - \Pi(\omega, k, p_F) = 0 \quad (1)$$

in the complex plane of the pion frequency  $\omega$ . In (1)  $\Pi$  is the pion polarization operator (pion self-energy) in the matter. The consideration in the complex  $\omega$ -plane allows us to obtain additional information about well-known solutions.

The main content is as follows. We consider excitations with quantum numbers  $0^-$  in symmetrical nuclear matter. At the equilibrium density there are three branches of solutions of (1). When the density is larger than critical one ( $\rho > \rho_c$ ) the fourth branch appears on the physical sheet.

The equation (1) has logarithmic cuts on the physical sheet of the complex  $\omega$ -plane, determined by the structure of the polarization operator  $\Pi$ . Different branches of solutions are considered on physical and unphysical sheets of the complex  $\omega$ -plane. With the change of  $k$  they move from physical to unphysical sheet (and backward) through the cuts. Below, to explain the obtained results, we deal with the case when isobar width in medium is equal to that in vacuum, i.e. 115 MeV. In this case all solutions of (1) and certain cuts move from the real (or imaginary) axis to the complex plane. This helps us to trace the  $k$ -dependence of the solutions. For certain important cases the influence of  $\Gamma_\Delta$  on the behaviour of  $\omega_i(k)$  is studied.

The well-known branches of solutions (1) are: 1) spin-isospin sound branch  $\omega_s(k)$ ; 2) pion branch  $\omega_\pi(k)$ ; 3) isobar branch  $\omega_\Delta(k)$ . At  $0 \leq k \leq k_f$  they are located on the physical sheet (the momentum  $k_f$  is different for each branch), then with further increase of  $k$  they move to unphysical sheet across the cuts. For these branches  $\text{Re}(\omega_i^2) > 0$  everywhere on the physical sheet.

Our investigations show that there is the whole set of solutions at unphysical sheets. With increasing density certain solutions come to the physical sheet. In such a way the fourth branch,  $\omega_c(k)$ , appears on the physical sheet at  $p_F \geq 283$  MeV<sup>1</sup>. Below  $\omega_c(k)$  is referred as the condensate branch. At  $k = 0$   $\omega_c(k)$  is located at the same point as  $\omega_\pi(k)$ ; with increasing of  $k$  the branch goes onto the unphysical sheet. At some  $k = k_1$  it appears on the physical sheet and at  $k = k_2$  leaves it for the same unphysical sheet. The values of  $k_1$  and  $k_2$  depend on the density. At critical density,  $\rho_c$ , corresponding to  $p_F = 283$  MeV ( $\rho_c \simeq 1.2\rho_0$ ) there is the equality  $k_1 = k_2 = 1.8m_\pi$ . It is  $\omega_c$  which obeys the inequality  $\text{Re } \omega_c^2 \leq 0$ . All branches depend on the isobar width: at  $\Gamma_\Delta = 0$  the branch  $\omega_c(k)$  is pure imaginary and  $\omega_c^2 \leq 0$ . Recall that  $\rho_0$  is the equilibrium density of the matter,  $\rho_0 = 2p_{F0}^3/3\pi^2$ ,  $p_{F0} = 268$  MeV.

The paper is organized as follows. In section 2 the particle-hole polarization operator  $\Pi$  is considered in the complex  $\omega$ -plane. Then the branches of solutions of the pion dispersion equation (1) are presented on the physical and unphysical sheets. It is shown how the branches of solutions go across the logarithmic cuts in the complex plane. The condensate branch  $\omega_c$  is shown in details at different densities  $\rho$  and isobar width  $\Gamma_\Delta$ .

## 2 Polarization operator and its singularities

Here we write down the formulae for the polarization operator used. Our expressions, as is shown below, differ in some points from the well-known expressions [1, 2]. Only  $S$ - and  $P$ -waves of the  $\pi NN$  ( $\pi N\Delta$ ) interactions are taken into account. In this case  $\Pi$  is the sum of scalar,  $\Pi_S$ , and vector,  $\Pi_P$ , terms:

$$\Pi(\omega, k) = \Pi_S(\omega, k) + \Pi_P(\omega, k) . \quad (2)$$

The scalar polarization operator  $\Pi_S$  is constructed using linear PCAC equation obtained by Gell-Mann–Oakes–Renner (GMOR) [5] for the pion mass squared in the matter:

$$m_\pi^{*2} = -\frac{\langle NM|\bar{q}q|NM\rangle(m_u + m_d)}{2f_\pi^{*2}} . \quad (3)$$

---

<sup>1</sup>For our values of the parameters, which are presented below.

The value  $\kappa = \langle NM|\bar{q}q|NM \rangle$  is the scalar quark condensate calculated in nuclear matter [6];  $m_u, m_d$  are masses of the current  $u$ - and  $d$ -quarks;  $f_\pi^*$  is the pion decay constant in medium. Here we put  $f_\pi^* = f_\pi = 92$  MeV (more details can be found in [6]).

The scalar quark condensate  $\kappa$  can be expanded in a power series with respect to  $\rho$  [6, 7]

$$\kappa = \kappa_0 + \rho \langle N|\bar{q}q|N \rangle + \text{terms with higher degrees of } \rho, \quad (4)$$

where  $\kappa_0$  is the value of scalar quark condensate in vacuum,  $\kappa_0 = -0.03$  GeV<sup>3</sup>;  $\langle N|\bar{q}q|N \rangle$  is the matrix element for scalar quark condensate in nucleon,  $\langle N|\bar{q}q|N \rangle \simeq 8$ . In this place it is enough to keep the first two terms in (4), this correspond to the gas approximation for  $\kappa$  [7]. Then we get from (3)

$$m_\pi^{*2} = m_\pi^2 - \rho \frac{\langle N|\bar{q}q|N \rangle (m_u + m_d)}{2f_\pi^2}. \quad (5)$$

On the other hand, in the dispersion equation (1)  $m_\pi^{*2}$  is defined as

$$m_\pi^{*2} = m_\pi^2 + \Pi(\omega, k = 0). \quad (6)$$

Whilst  $\Pi_P(k = 0) = 0$ , we get from (5) and (6) the following form for  $\Pi_S$ :

$$\Pi_S = -\rho \frac{\langle N|\bar{q}q|N \rangle (m_u + m_d)}{2f_\pi^2}. \quad (7)$$

The P-wave polarization operator  $\Pi_P$  can be written following the papers [1, 2, 8, 9] as a sum of nucleon and isobar polarization operators

$$\Pi_P = \Pi_N + \Pi_\Delta. \quad (8)$$

Here  $\Pi_N(\Pi_\Delta)$  is equal to the sum of the nucleon-hole and isobar-hole loops without pion in the intermediate states [1, 2, 8]:

$$\begin{aligned} \Pi_N &= \Pi_N^0 \frac{1 + (\gamma_\Delta - \gamma_{\Delta\Delta}) \Pi_\Delta^0/k^2}{E}, \quad \Pi_\Delta = \Pi_\Delta^0 \frac{1 + (\gamma_\Delta - \gamma_{NN}) \Pi_N^0/k^2}{E}, \\ E &= 1 - \gamma_{NN} \frac{\Pi_N^0}{k^2} - \gamma_{\Delta\Delta} \frac{\Pi_\Delta^0}{k^2} + (\gamma_{NN}\gamma_{\Delta\Delta} - \gamma_\Delta^2) \frac{\Pi_N^0 \Pi_\Delta^0}{k^4}. \end{aligned} \quad (9)$$

The expressions for the nucleon-hole loop,  $\Pi_N^0$ , is as follows:

$$\Pi_N^0(\omega, k) = \text{Sp} \int \frac{d^3 p}{(2\pi)^3} \Gamma_{\pi NN}^2 \left[ \frac{\theta(p - p_F)\theta(p_F - |\vec{p} + \vec{k}|)}{E_{\vec{p} + \vec{k}} - E_p - \omega} + \frac{\theta(p_F - p)\theta(|\vec{p} + \vec{k}| - p_F)}{E_p - E_{\vec{p} + \vec{k}} + \omega} \right]. \quad (10)$$

Here  $E_p = p^2/2m^*$ . The expression for  $\Pi_\Delta^0$  is analogous.

The  $\pi NB$  vertex  $\Gamma_{\pi NB}$  with  $B$  labelling nucleon or  $\Delta$ -isobar is

$$\Gamma_{\pi NB} = \Gamma_{\pi NB}^0 d_B(k), \quad (11)$$

$$\Gamma_{\pi NN}^0 = i \frac{g_A}{\sqrt{2} f_\pi} \chi^*(\vec{\sigma} \vec{k}) \chi, \quad \Gamma_{\pi N\Delta}^0 = f_{\Delta/N} i \frac{g_A}{\sqrt{2} f_\pi} \chi^{*\alpha} (\vec{S}_\alpha^+ \vec{k}) \chi, \quad (12)$$

where  $\chi$  is nucleon 2-spinors,  $\vec{\sigma}$  is nucleon spin,  $\vec{S}^+$  turns the spin  $3/2$  into  $1/2$ . In order to take into account the non-zero baryon size, the vertex  $\Gamma_{\pi NB}^0$  is multiplied by the form factor  $d_B(k)$  taken in the form  $d_B = (1 - m_\pi^2/\Lambda_B^2)/(1 + k^2/\Lambda_B^2)$ .

The constants  $\gamma_{NN}, \gamma_\Delta, \gamma_{\Delta\Delta}$  are

$$\gamma_{NN} = C_0 g'_{NN} \left( \frac{\sqrt{2} f_\pi}{g_A} \right)^2, \quad \gamma_\Delta = \frac{C_0 g'_{N\Delta}}{f_{\Delta/N}} \left( \frac{\sqrt{2} f_\pi}{g_A} \right)^2, \quad \gamma_{\Delta\Delta} = \frac{C_0 g'_{\Delta\Delta}}{f_{\Delta/N}^2} \left( \frac{\sqrt{2} f_\pi}{g_A} \right)^2,$$

where  $C_0$  is the normalization factor ( $C_0 = \pi^2/(p_F m^*)$ ) and  $g'$ s are the constants of the effective quasi-particle-quasi-hole interaction in nuclear matter [1, 2]. The calculation results are given for the following set of parameters [1, 2, 8] :

$$f_{\Delta/N} \simeq 2, \quad \Lambda_N = 0.667 \text{GeV}, \quad \Lambda_\Delta = 1 \text{GeV}, \quad g_A = 1, \quad f_\pi = 92 \text{MeV}, \quad (13)$$

$$g'_{NN} = 1.0, \quad g'_{N\Delta} = 0.2, \quad g'_{\Delta\Delta} = 0.8.$$

When the parameters  $f_{\Delta/N}, g', \Lambda_B$  vary within the experimentally acceptable limits the dispersion equation solutions change quantitatively but not qualitatively.

Later on, we can perform integration in (10) in two ways.

1. To integrate separately the first and the second terms. In this way there appears the expression for  $\Pi_N^0$  as follows:

$$\Pi_N^0(\omega, k) = -4 \left( \frac{g_A}{\sqrt{2} f_\pi} \right)^2 k^2 [\Phi_N(\omega, k) + \Phi_N(-\omega, k)] d_N^2(k), \quad (14)$$

$$\begin{aligned} \Phi_N(\omega, k) = & \frac{m^*}{k} \frac{1}{4\pi^2} \left( \frac{-\omega m^* + kp_F}{2} - \omega m^* \ln \left( \frac{\omega m^*}{\omega m^* - kp_F + k^2/2} \right) \right. \\ & \left. + \frac{(kp_F)^2 - (\omega m^* - k^2/2)^2}{2k^2} \ln \left( \frac{\omega m^* - kp_F - k^2/2}{\omega m^* - kp_F + k^2/2} \right) \right) \end{aligned} \quad (15)$$

at  $0 \leq k \leq 2p_F$ . At  $k \geq 2p_F$   $\Phi_N(\omega, k)$  is Migdal's function:

$$\Phi_N(\omega, k) = \frac{1}{4\pi^2} \frac{m^{*3}}{k^3} \left[ \frac{a^2 - b^2}{2} \ln \left( \frac{a+b}{a-b} \right) - ab \right] \quad (16)$$

where  $a = \omega - (k^2/2m^*)$ ,  $b = kp_F/m^*$ . Consider now which cuts has the polarization operator  $\Pi_N^0(\omega, k)$  (14)–(16) in the  $\omega$ -plane. We can see that at  $k \leq 2p_F$  there are two cuts (define them as *I* and *II*). They are related to the first and second logarithms in (15). The cuts are situated within the intervals:

$$I : \quad 0 \leq \omega \leq \frac{kp_F}{m^*} - \frac{k^2}{2m^*}, \quad II : \quad \frac{kp_F}{m^*} - \frac{k^2}{2m^*} \leq \omega \leq \frac{kp_F}{m^*} + \frac{k^2}{2m^*}. \quad (17)$$

Since  $\Pi_N^0$  is symmetrical under the replacement  $\omega \leftrightarrow -\omega$ , the cuts of  $\Phi_N(-\omega, k)$  are placed symmetrically on the negative semiaxis. Thus  $\Pi_N^0$  has four cuts in the complex  $\omega$ -plane, they are shown in Fig.1.

2. The other way of integration in (10) gives a well-known expression of  $\Pi_N^0$  through Migdal's functions. To follow it, let us do a substitution in (10)  $\theta(p-p_F) \rightarrow 1-\theta(p_F-p) = 1-n(p)$ . Then, after the integration,  $\Phi_N(\omega, k)$  takes a well-known form (16) for all values of  $k$  [1, 2, 8]. Undoubtedly, the expression (14) is the same for both integration ways. Now  $\Pi_N^0$  has not four cuts in  $\omega$ -plane but two (overlapping). It can be seen from the expressions (10), (15), that the cut *I* is the sum of two overlapping cuts. The search for dispersion equation solutions becomes more convenient and obvious when we work with one cut but not with two overlapping ones. It is difficult to follow the solution in the case 2, therefore we use equations (14)–(16) for  $\Pi_N^0$ .

Now let us turn to the polarization operator  $\Pi_\Delta^0$ , which is the isobar–nucleon-hole loop. Since the isobar Fermi surface is absent at the nuclear densities and isobar momentum is unrestricted, there is no problem discussed above and  $\Pi_\Delta^0(\omega, k)$  reads:

$$\Pi_\Delta^0 = -\frac{16}{9} \left( \frac{g_A}{\sqrt{2} f_\pi} \right)^2 f_{\Delta/N}^2 k^2 \left[ \Phi_\Delta(\omega, k) + \Phi_\Delta(-\omega, k) \right] d_\Delta^2(k). \quad (18)$$

The function  $\Phi_\Delta(\omega, k)$  is expressed through Migdal's functions (16) with  $a = \omega - (k^2/2m^*) - \Delta m$ ,  $b = kp_F/m^*$ . The mass difference,  $\Delta m = m_\Delta - m$ , is the following:  $\text{Re}(\Delta m) = 292$  MeV and  $\text{Im}(\Delta m) = -\Gamma_\Delta/2$ . The cuts of  $\Phi_\Delta^0(\omega, k)$  are shown in Fig.1. At  $\omega \geq 0$  the cut is in the interval

$$\frac{k^2}{2m^*} + \Delta m - \frac{kp_F}{m^*} \leq \omega \leq \frac{k^2}{2m^*} + \Delta m + \frac{kp_F}{m^*}. \quad (19)$$

The cut is shifted into the complex plane in the value  $-i\Gamma_\Delta/2$ .

In this paper Landau equation [10] is used for the nucleon effective mass

$$m^* = \frac{m}{1 + (2mp_F/\pi^2)f_1}. \quad (20)$$

Unknown parameter  $f_1$  is fixed by the condition  $m^*(p_F = p_{F0}) = 0.8m$ .

### 3 Solutions of the dispersion equation

In this section the solutions of the dispersion equation (1) are presented. The solution branch  $\omega_c$  emerges on the physical sheet of the complex  $\omega$ -plane at  $p_F = 283$  MeV for the parameter values (13). The figures for the zero sound branch  $\omega_s(k)$ , pion branch  $\omega_\pi(k)$  and isobar branch  $\omega_\Delta(k)$  are presented for  $\Gamma_\Delta = 115$  MeV at  $p_F = 268$  and  $290$  MeV (i.e. at the equilibrium density and at density slightly larger than critical one). Some special cases, with the other values of  $p_F$  and  $\Gamma_\Delta$ , are considered as well.

**Branch  $\omega_s(k)$ .** (Fig.2a) The branch  $\omega_s(k)$  is shown for  $p_F = 268$  and  $290$  MeV (curves 1 and 2 correspondingly). The branch begins at  $\omega_s(k = 0) = 0$ , then while  $k$  increases, moves practically along the real axis. At  $k_f = 0.430m_\pi$  for  $p_F = 290$  MeV (at  $k_f = 0.436m_\pi$  for  $p_F = 268$  MeV) goes under the cut  $II$  (17), this corresponds to the decay of  $\omega_s$  into real nucleon and the hole.

**Branch  $\omega_\Delta(k)$ .** (Fig.2b) The isobar branch  $\omega_\Delta(k)$  begins at  $\omega = \Delta m$  at  $k = 0$  and ends on the isobar cut (19) at  $k_f = 5.1m_\pi$  for  $p_F = 268$  MeV ( $k_f = 4.8m_\pi$  for  $p_F = 290$  MeV).

**Branch  $\omega_\pi(k)$ .** (Fig.2c) The pion branch starts at  $k = 0$  in  $\omega_\pi = m_\pi^*$  (see (5),(6)). The beginning of  $\omega_\pi(k = 0)$  is shifted to the smaller than  $m_\pi$  values when GMOR [5] is used to determine  $m_\pi^*$ . The pion branch ends on physical sheet under the isobar cut, this corresponds to the decay of pion into isobar and nucleon hole. It takes place at  $k_f = 3.5m_\pi$  for  $p_F = 268$  MeV ( $k_f = 3.8m_\pi$ ,  $p_F = 290$  MeV).

**Branch  $\omega_c(k)$ .** (Fig.2d, 3a,b) While the density increases one more branch of solutions,  $\omega_c(k)$ , appears on the physical sheet. It emerges at  $p_F \geq 283$  MeV when parameter values (13) are used. In Fig.2d the pion branch  $\omega_\pi(k)$  and condensate branch  $\omega_c(k)$  are presented at  $p_F = 290$  MeV. The dashed piece of  $\omega_c(k)$  belongs to the upper unphysical sheet of the logarithmic cut  $I$  (17) (Fig.1). The branch  $\omega_c(k)$  starts at  $k = 0$  at the same point as  $\omega_\pi(k)$  and moves onto the unphysical sheet; at  $k = k_1 = 1.3m_\pi$  the branch goes down to the physical sheet and at  $k = k_2 = 2.3m_\pi$  moves back to the same unphysical sheet. In the momentum interval  $(k_1, k_2)$  one can follow over all the branches shown in Fig.2 and check that  $\omega_c$  does not belong to any branches studied before  $(\omega_s, \omega_\pi, \omega_\Delta)$ .

The branch  $\omega_c$  depends on the isobar width  $\Gamma_\Delta$ . Decreasing the isobar width we see that the isobar cuts move to the real axis and  $\omega_s$ ,  $\omega_\pi$  and  $\omega_\Delta$  have smaller imaginary parts. When  $\Gamma_\Delta = 0$  the branches  $\omega_s$ ,  $\omega_\pi$  and  $\omega_\Delta$  are real. On the contrary,  $\omega_c(k)$  moves to the imaginary axis with decreasing  $\Gamma_\Delta$  (Fig.3a). At  $\Gamma_\Delta = 0$  we have pure imaginary solutions on the physical sheet:  $\omega_c^2 \leq 0$ .

In Fig.3b the branch  $\omega_c(k)$  is shown at the different densities:  $p_F = 280, 290, 300, 360$  MeV. When  $p_F = 280$  MeV the whole branch (curve 1) is located on unphysical sheet. At  $p_F = 283$  MeV the branch touches the real axis (not shown). For  $p_F > 283$  Mev the part of  $\omega_c(k)$  in the interval  $(k_1, k_2)$  is placed on the physical sheet.

It was shown in paper [6] that the appearance of  $\omega_c$  on the physical sheet results not only in pion condensation but in restoration of chiral symmetry in the nuclear matter at critical density as well.

## 4 Conclusion

In the paper the solutions of pion dispersion equation are considered in details in the complex  $\omega$ -plane. It is shown that, besides the well-known solutions with quantum numbers  $0^-$  (zero spin-isospin sound, pion and isobar waves), there exists the fourth branch  $\omega_c(k)$ . It is the branch which obeys the condition  $\omega_c^2 \leq 0$ , therefore it is responsible for instability of the ground state. Such instability can indicate the beginning of 'pion condensation'.

We demonstrate that at the density less than critical one,  $\rho < \rho_c$  the branch  $\omega_c(k)$  is situated on unphysical sheet and at  $\rho \geq \rho_c$  it comes on physical one.

## Acknowledgments

I am grateful to M.G. Ryskin for the important and fruitful discussions during the work. I thanks E.G. Drukarev and E.E. Saperstein for useful discussions. This work was supported by RFFI grant 96-15-96764.

## References

- [1] A.B. Migdal, Rev.Mod.Phys., 50 (1978) 107;  
JETF 34 (1972) 1184.
- [2] A.B. Migdal, D.N. Voskresenskii, E.E. Saperstein, M.A. Troitskii, Pion degrees of freedom in nuclear medium, Nauka , Moskow,1991.
- [3] G.E. Brown, W. Weise, Phys.Rep. 27 (1976) 1.
- [4] D.-O. Backman, G.E. Brown, J.A. Niskanen, Phys.Rep. 124 (1985) 1.
- [5] M.Gell-Mann, R. Oakes, B. Renner, Phys. Rev. 175 (1968) 2195.
- [6] E.G. Drukarev, M.G. Ryskin, V.A. Sadovnikova, Eur.Phys.J. A 4 (1999) 171.
- [7] E.G.Drukarev and E.M.Levin, JETP Lett. 48 (1988) 338.
- [8] T. Ericson, W. Weise, Pions and nuclei, Clarendon Press, 1988.
- [9] W.H. Dickhoff, A. Faessler, J. Meyr-ter-Vehn, and H. Muthner, Phys.Rev. C 23 (1981) 1154.
- [10] L.D.Landau, JETP 30 (1956) 1058.

## 5 Figure captions

Fig.1. The cuts on the physical sheet of the complex  $\omega$ -plane of polarization operators  $\Pi_N^0$ ,  $\Pi_\Delta^0$ , corresponding to equations (14), (17), (18), (19). The cuts are presented at  $p_F = 290$  MeV,  $k = m_\pi$ .

Fig.2. Branches of solutions of (1) in the complex  $\omega$ -plane. Curves 1 and 2 stand for  $p_F = 268, 290$  MeV, correspondingly. The dashed pieces of curves are situated on unphysical sheets. a) Zero spin-isospin sound branch  $\omega_s(k)$ . The curves are presented up to  $1.6m_\pi$ . b) The isobar branch  $\omega_\Delta$ . The horizontal dashed line is a logarithmic cut (19) for  $p_F = 290$  MeV at momentum  $k$  when  $\omega_\Delta(k)$  is on the cut. c) The pion branch  $\omega_\pi$ . The horizontal dashed line is a logarithmic cut (19) for  $p_F = 290$  MeV at momentum  $k$  when  $\omega_\pi$  is on the cut. d) The total picture at  $p_F = 290$  MeV for pion branch  $\omega_\pi(k)$  and condensate branch  $\omega_c(k)$ .

Fig.3. Condensate branch  $\omega_c$  in the complex  $\omega$ -plane. Here the dashed pieces of branches are on the physical sheet, but solid lines belong to unphysical sheet. a) The branch  $\omega_c$  is presented at  $p_F = 290$  MeV for different values of isobar width:  $\Gamma_\Delta = 0, 10, 50, 115$  MeV (curves 1,2,3,4, correspondingly);  $\omega_c(k = 0) = 0.744m_\pi$ . b) The branch  $\omega_c$  is presented at  $\Gamma_\Delta = 115$  MeV for different values of Fermi momenta  $p_F = 280, 290, 300, 360$  MeV (curves 1,2,3,4, correspondingly). For  $p_F = 300$  and  $360$  MeV only the part of the branch, which is placed on the physical sheet, is shown (the curves 3 and 4). The whole branch for  $p_F = 280$  MeV (curve 1) is on unphysical sheet.

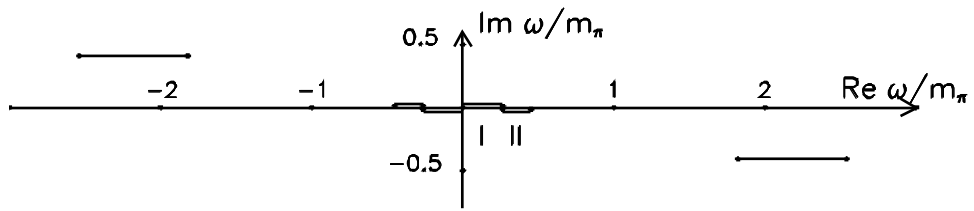


Figure 1:

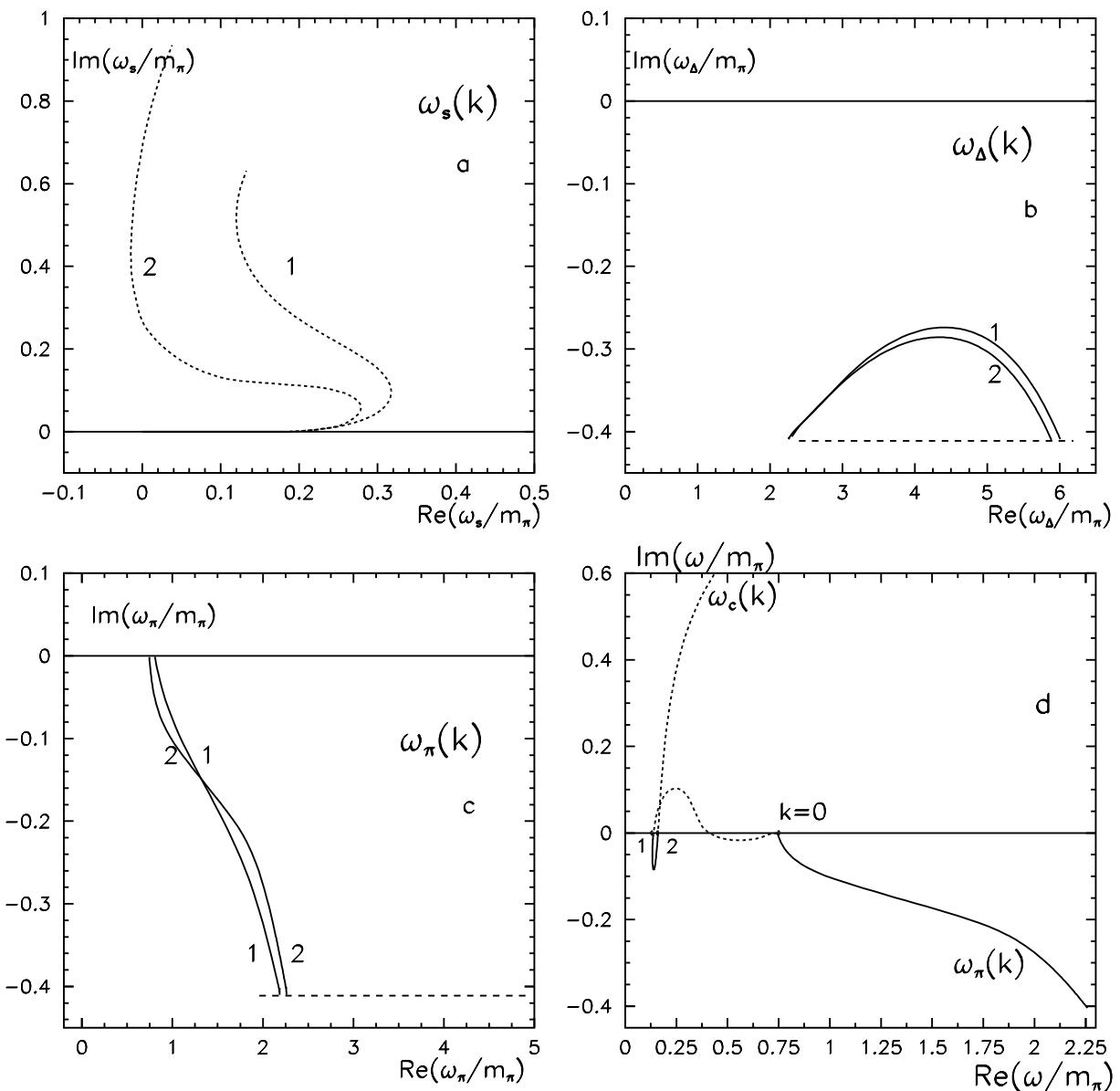


Figure 2:

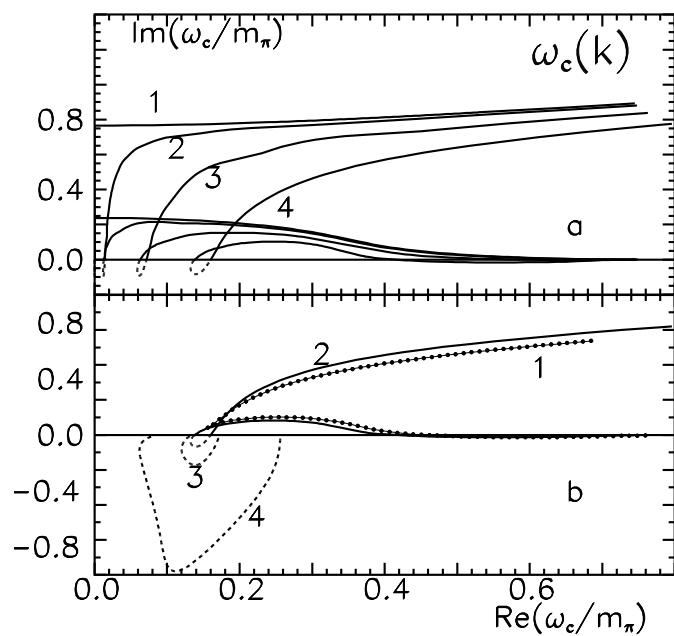


Figure 3: